Magnetic and electrostatic separation to increase tin in heavy minerals concentrate of Rondônia Tin Province

Gustavo Simões de Araújo [1]
Júlia Guimarães Sanches [2]
Maurício Guimarães Bergerman [2]*
Guilherme José Ramos de Oliveira [1]
Daniela Gomes Horta [1]

Abstract

The Rondônia Tin Province (RTP) reserves display several valuable minerals, such as cassiterite (SnO_2), columbite-tantalite ($(Fe,Mn)(Nb,Ta)_2O_6$), and ilmenite ($FeTiO_3$). This work evaluated the use of magnetic and electrostatic separation of heavy minerals concentrate from gravity separation of an RTP industrial plant to targeting a high grade cassiterite concentrate (>55% of Sn) for metallurgical use. Two samples were collected from the concentrate of shaking tables and spirals. The samples were characterized by determining their chemical composition and particle size distribution. Dry magnetic separation was investigated by increasing the field intensities, followed by electrostatic separation in nonmagnetic products. Wet magnetic separation was also investigated by increasing the field intensities using a scavenger stage. Dry magnetic separation followed by electrostatic separation was the most promising concentration strategy. Dry magnetic separation increased the Sn content from 39.24%-35.57% in the gravimetric separation concentrates to 57.21%-45.15%, with metallurgical recoveries of 87.33%-90.23%. In addition, electrostatic separation elevated the Sn content even more to 66.82%-71.54%, with metallurgical recovery of 75.67%-78.60%, respectively.

Keywords: Magnetic separation; Electrostatic separation; Heavy minerals; Cassiterite.

1 Introduction

The Rondônia Tin Province (RTP), located in the North of the state of Rondônia, Brazil, comprises an important source of cassiterite (SnO_2), columbite-tantalite ($(Fe,Mn)(Nb,Ta)_2O_6$), ilmenite ($FeTiO_3$), and wolframite ($(Fe,Mn)WO_4$) [1]. Zircon ($ZrSiO_4$), topaz ($Al_2(F,OH)_2SiO_4$), and rare earth element (REE) bearing minerals can also be found [2].

Primary tin (Sn) mineralization occurs in greisen, pegmatite, and quartz veins related to granitic intrusions of the Rapakivi type [1,3]. Conversely, secondary mineralization takes place in alluvial sedimentary deposits (placer type), called paleoalluviums, forming concentrations of heavy minerals along ancient drainages. There has also been mineralization in recent alluvium, colluvium, and eluvium, located close to primary mineralization. Secondary deposits account for most of the ore processed in the RTP [4,5].

The RTP valuable minerals display high specific weights [6] and usually liberate at coarser sizes [7], which justifies the use of gravimetric concentration equipment, such as jigs, spirals, and shaking tables [8]. However, in some plant operations, it is hard to reach concentrates with the specification of 55% Sn.

The excess of certain contaminants hinders the metallurgical process. For instance, iron-bearing minerals, such as ilmenite and columbite-tantalite, form the hard head, a Fe-Sn-Si alloy, reducing the metallurgical recovery. Silica and aluminium negatively influence the formation of slag [9]. These impacts bring an increase in the use of electric energy, loss of tin to slag, and accelerated wear of the internal coatings and electrodes of electric furnaces [9].

Considering the low magnetic susceptibility of cassiterite and high magnetic susceptibility of columbite-tantalite and ilmenite as shown in Table 1 [10], magnetic separation is an alternative aimed at improving Sn recovery and reducing iron-bearing mineral content. Some RTP plant operations conduct dry magnetic separation in cross-belts, drums, or rare earth rolls. Wet magnetic and electrostatic separation are currently not industrially used [11]. It is important to highlight that the electrostatic separation operation in the Amazon Forest, were the RTP is located, is challenging due to the region's high atmospheric humidity.

Campos and Delboni [12] applied magnetic separation in rare earth high-intensity drums, followed by electrostatic

[1]*Grupo de Pesquisa em Processamento Mineral, GPPM, Núcleo de Engenharia de Minas, Universidade Federal de Alfenas, UNIFAL-MG, Poços de Caldas, MG, Brasil.*
[2]*Laboratório de Tratamento de Minérios e Resíduos Industriais, LTM, Departamento de Engenharia de Minas de Petróleo, Escola Politécnica, Universidade de São Paulo, USP, São Paulo, SP, Brasil.*

**Corresponding author: mbergerman@usp.br*

separation, to concentrate a gravimetric product from the Pitinga mine located in the Amazon. They achieved a cassiterite concentrate displaying 51.7% Sn with a metallurgical recovery of 77.5%. Buchmann et al. [13] reduced the Fe grade from nearly 30% to less than 5% using dry magnetic separation by a drum-type magnetic separator in complex tin-bearing skarn ore.

Abd El-Rahman et al. [14] optimized a tin concentration plant operation using a shaking table and dry high-intensity magnetic separator. The magnetic separation increased the SnO_2 grade from 13,2% to 90,67%. Zhang et al. [15] investigated the effect of roasting, followed by wet magnetic separation, to recover magnetite-type tin-bearing tailings. A magnetic concentrate containing 0.091% Sn was obtained, and tin was enriched in nonmagnetic materials.

Our objective was to elevate the Sn content of a cassiterite gravimetric concentrate to more than 55% using dry magnetic separation, followed by electrostatic or wet magnetic separation.

2 Materials and methods

2.1 Sample preparation and characterization

Figure 1 shows the processing flowsheet of the RTP's secondary cassiterite mine (alluvium), where the gravimetric concentrate was collected. The process includes slurring, classification, and concentration operations. After disaggregation with water jets, the coarse fraction is separated using a rotary sieve (trommel), then comminuted with a hammer mill down to 25.4 mm. The preparation ends by removing the -2.5 mm fraction using an inclined vibrating screen. Gravity concentration is performed in Panamerican jigs, spirals, and shaking tables, resulting in concentrates with Sn content ranging from 30% to 76%.

Two samples of approximately 30 kg, comprising the concentrate of spirals or shaking tables (Figure 1), were collected. The samples were homogenized in longitudinal piles and quartered to feed characterization and concentration.

Table 1. Magnetic field (T) and conductivity required for the separation of the main minerals from the RTP

RTP Minerals	Formula	Magnetism	Mag. Field (T)	Conductivity
Ilmenite	$FeTiO_3$	Mod. Magnetic	0.5 to 1.0	Conductor
Columbite/Tantalite	$(Fe,Mn)(Nb,Ta)_2O_6$	Weakly Magnetic	1.0 to 1.8	Conductor
Cassiterite	SnO_2	V. Weakly Magnetic	> 1.8	Conductor
Monazite	(La,Ce,Nd) PO4	V. Weakly Magnetic	> 1.8	Non-Conductive
Zircon	$Zr(SiO_4)$	V. Weakly Magnetic	> 1.8	Non-Conductive
Quartz	SiO_2	Non-Magnetic	N.A	Non-Conductive
Topaz	$Al_2(SiO_4)(F,OH)_2$	Non-Magnetic	N.A	Non-Conductive

Modified from Sampaio et al. [10].

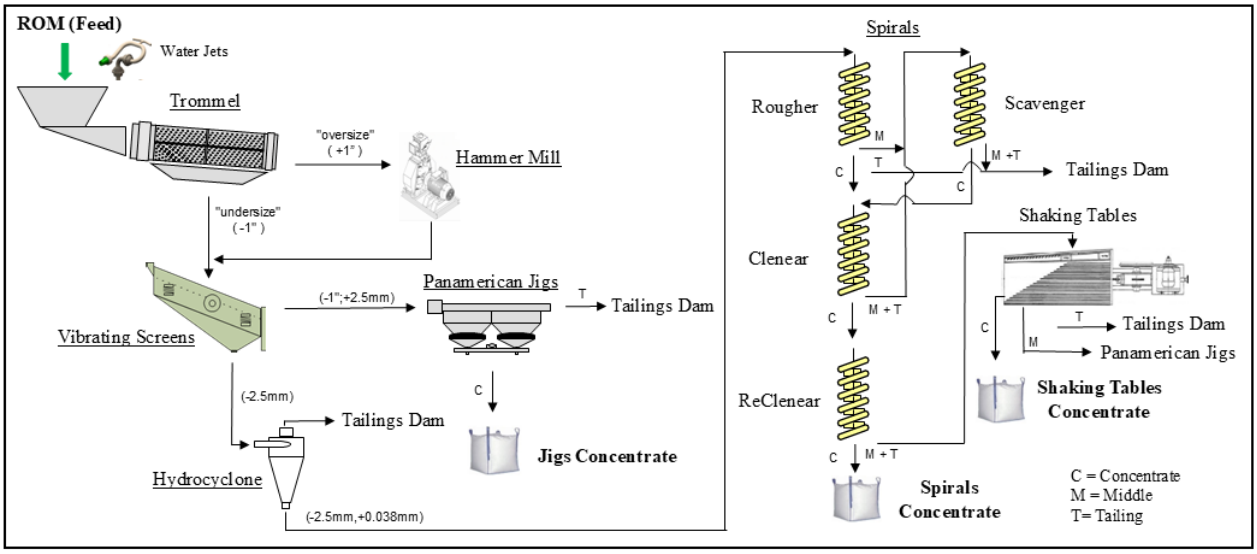

Figure 1. Simplified flowsheet of the cassiterite processing plant.

The particle size distribution was determined by wet sieving in 2.36, 1.70, 0.60, 0.15, 0,075, 0.045, and 0.038 mm. Chemical analyses were conducted in each size fraction. X-ray fluorescence (XRF) (Panalytical Epsilon 4, using the ITAK© 703 standards) was used to determine the Al_2O_3, SiO_2, TiO_2, Fe_2O_3, ZrO_2, Nb_2O_5, and Ta_2O_5 oxides. The Sn content was determined by titration (iodometry), according to the method routinely used at the RTP.

2.2 Dry magnetic separation and electrostatic separation

The samples were dried at 100 °C for 24 hours. First, the fraction -0,150 +0,075 µm was submitted to magnetic separation using the increasing field intensities shown in Figure 2A in the Frantz magnetic separator (Frantz LB-1). The lateral and longitudinal inclinations were 15° and 13°, respectively. This equipment is a laboratory magnetic separator that operates in ideal conditions and is used to obtain the best possible metallurgical result experimentally. Thus, the results were used as a reference for further magnetic separation tests.

Next, dry magnetic separation experiments were conducted in (1) drum magnetic separators applying the magnetic fields of 0.15 T (Inbras HFRE 15x12) and 0.5 T (Inbras HFPRE 15×12) and in a (2) rare earth roll separator using 1.3 T (Inbras RE 5/04-1), as illustrated in Figure 2B. The drum and roll separators ' rotational speeds were 41.6 rpm and 110 rpm, respectively. The deflector inclinations were 0° and 13° for the drums and roll, respectively.

The nonmagnetic products of the experiments conducted at 1.3 T were dried and submitted to electrostatic separation (Inbras ES-14-OLS) at 20 kV, as illustrated in Figure 2C. Rougher and scavenger stages were conducted at a drum speed of 40 rpm, and the deflectors stayed at 10º.

2.3 Wet magnetic separation

Before concentration, the samples were sieved at 0.60 mm to remove coarse particles and prevent equipment obstruction. The wet magnetic separation tests were performed in a high-intensity magnetic separator (Inbras L-4) using a 3.8 mm matrix and 0.15, 0.6 and 1.20 T magnetic field (Figure 3A). The magnetic products of the last two fields were

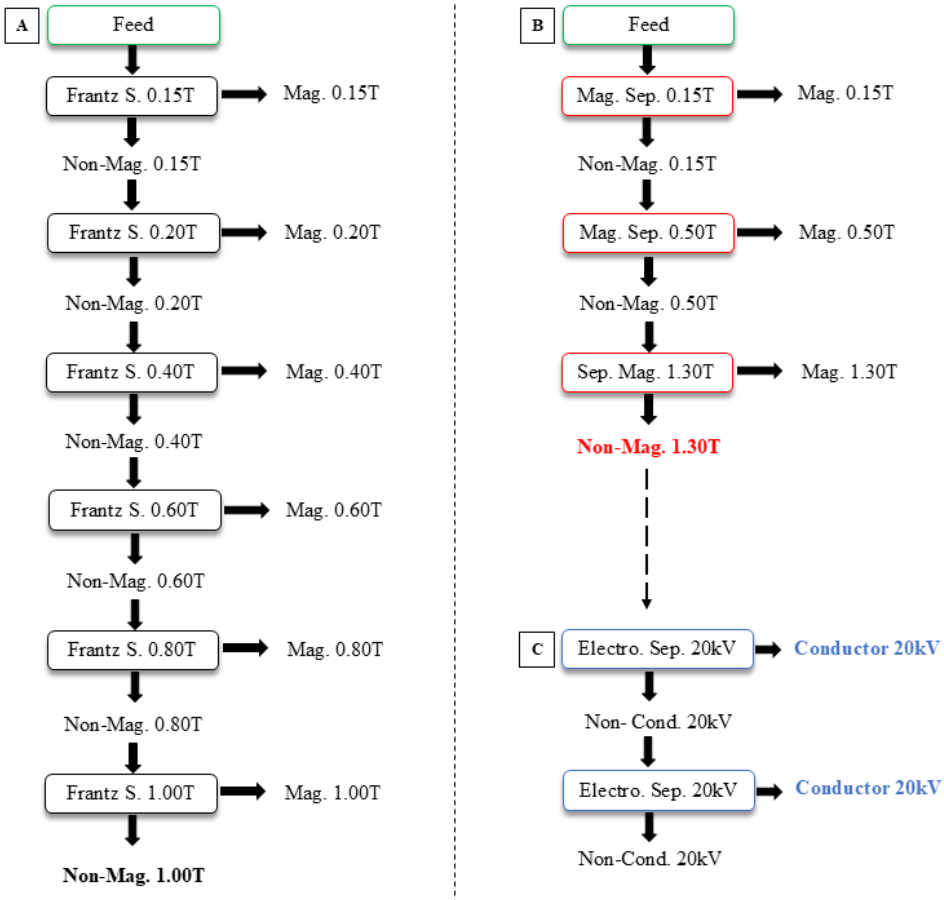

Figure 2. Flowchart of dry magnetic and electrostatic separation: (A) Frantz separator; (B) Drum separators and Rare Earth roll separators; (C) Electrostatic separation.

subjected to a scavenger step at the same field (Figure 3B). The separation at 0.15 T was manually performed by rotating a magnetic bar in the pulp ten times with ten rotations each time. The magnetic product was washed with 200 ml of water while keeping the field on. After the field was off, 500 ml of water was vigorously used to remove the magnetic product. The products were dried, weighed, quartered, and sent for chemical analysis.

3 Results and discussion

Figure 4 shows the particle size distribution of the shaking table and spiral concentrates. The particles are mostly present in the fraction -0.600+0.075 mm for both concentrates, showing a P80 at 0.40 mm and 0.42 mm for the shaking tables and the spirals concentrates, respectively. The shaking table concentrate has finer particles (49.82% below 0.15 mm) as compared to the spiral concentrate (28.08% below 0.15 mm).

Tables 2 and 3 show the main elements of the diverse size fractions for the shaking table and spiral concentrates, respectively. A physical concentration of Sn and Zr is observed in the fractions below 0.045 mm. However, the other analysed elements are concentrated in the median particle size fractions (0.600 to 0.045 mm).

The Sn content is higher in the shaking table concentrate (40.06%) than in the spiral (36.69%). The magnetic minerals, which can be identified by the Fe, Ti and Nb grades, are present in greater quantities in the shaking table concentrate. The spiral concentrate displays higher Al and Si contents, being twice as high as that observed in the shaking table concentrate, which justifies the lower Sn content.

Figure 5 shows the performance of the concentration strategies in terms of mass recovery versus Sn content. The magnetic separation in the Frantz equipment shows an ideal situation of the maximum possible separation between magnetic and nonmagnetic products. At 0.4 T, the Sn content/recovery was 56.37%/90.16% for the shaking table concentrate and 43.02/90.52% for the spiral concentrate.

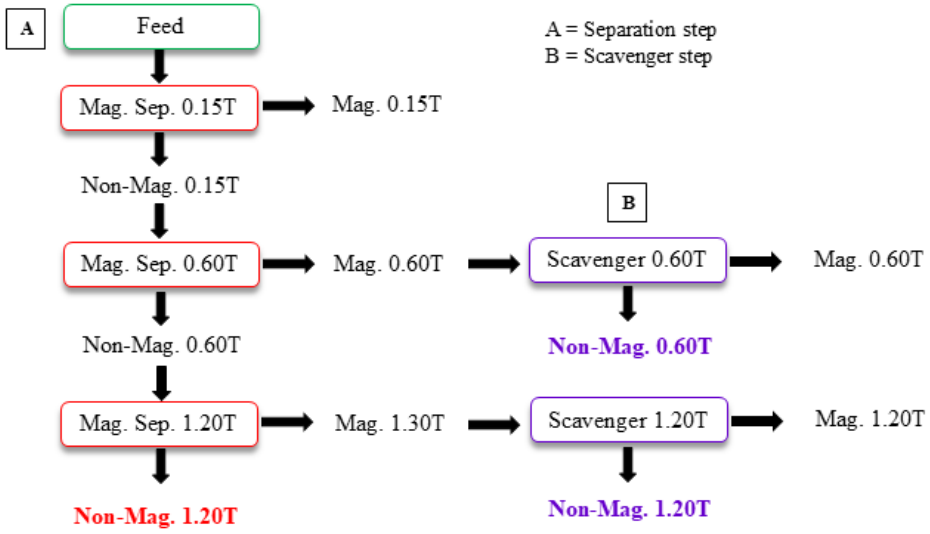

Figure 3. Flowchart of wet magnetic separation tests in different strategies: (A) Rougher (B) Scavenger

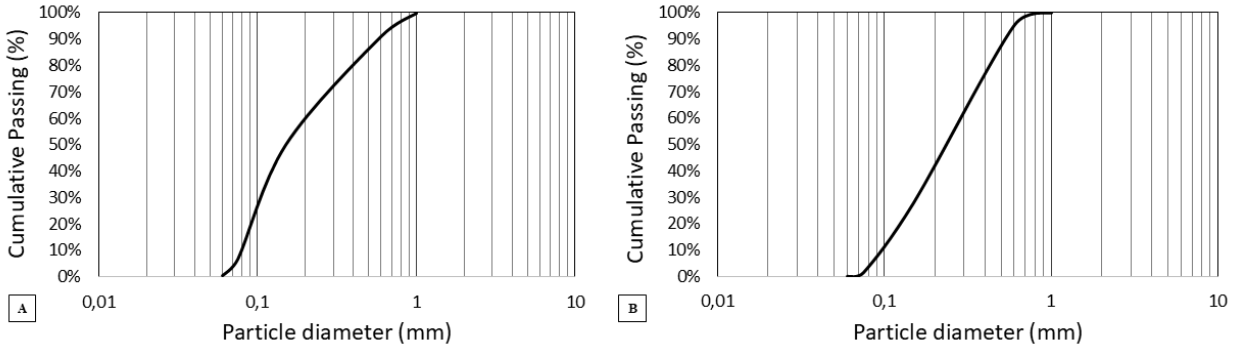

Figure 4. Particle size distribution of concentrate from (A) shaking tables and (B) spirals.

Table 2. Chemical composition by particle size ranges of the shaking tables concentrate

Sieves	Sn	Al_2O_3	SiO_2	TiO_2	Fe_2O_3	ZrO_2	Nb_2O_5	Ta_2O_5
(mm)	(%)	(%)	(%)	(%)	(%)	(%)	(%)	(%)
2.360	-	-	-	-	-	-	-	-
1.700	57.62	-	-	-	-	-	-	-
0.600	47.64	11.82	6.22	1.44	29.81	0.05	0.48	0.11
0.150	44.40	4.19	4.44	10.92	16.74	1.72	12.77	2.07
0.075	33.49	3.69	7.55	14.29	11.59	12.28	10.63	1.73
0.045	45.19	2.63	6.98	7.00	6.94	12.31	7.83	1.44
0.038	64.06	-	-	-	-	-	-	-
< 0.038	64.24	-	-	-	-	-	-	-
Global	40.06	5.95	5.70	9.10	18.87	4.31	8.78	1.44
Standard deviation	0.50	0.27	0.20	0.02	0.52	0.03	0.05	0.01
Standard error	0.36	0.19	0.14	0.02	0.37	0.02	0.04	0.01
0.150 - 0.075	38.78	3.93	6.04	12.65	14.08	7.16	11.66	1.89

Table 3. Chemical composition by particle size ranges of the spiral concentrate

Sieves	Sn	Al_2O_3	SiO_2	TiO_2	Fe_2O_3	ZrO_2	Nb_2O_5	Ta_2O_5
(mm)	(%)	(%)	(%)	(%)	(%)	(%)	(%)	(%)
2.360	-	-	-	-	-	-	-	-
1.700	62.21	-	-	-	-	-	-	-
0.600	35.58	17.14	9.22	0.82	31.93	0.12	0.66	0.12
0.150	40.25	17.20	11.41	5.98	10.38	1.41	8.31	1.24
0.075	27.31	19.01	14.58	8.92	8.34	9.55	6.44	0.95
0.045	36.84	6.46	8.03	7.20	8.15	15.08	7.13	1.06
0.038	53.63	-	-	-	-	-	-	-
< 0.038	50.75	-	-	-	-	-	-	-
Global	36.69	17.52	12.08	6.51	10.85	3.65	7.45	1.11
Standard deviation	1.27	0.55	0.48	0.54	0.55	0.18	0.14	0.02
Standard error	0.90	0.39	0.34	0.38	0.39	0.13	0.10	0.02
0.150 - 0.075	36.68	17.69	12.29	6.79	9.82	3.66	7.79	1.16

The Sn content does not increase in magnetic fields > 0,4 T, and there was a relevant reduction in recovery. Under this ideal condition, Mattioli [16] also found a limit of 0.4 T for the magnetic separation of an RTP tailing sample.

In conventional magnetic separation, regardless of the technique used (wet or dry), relevant Sn grade variation started in fields greater than 0.15 T, suggesting the absence of ferromagnetic minerals such as magnetite. Regarding the spiral concentrate, dry and wet magnetic separation yielded similar performance in increasing the Sn content. Under the most promising condition, the Sn grades were close to 45%, with metallurgical recoveries > 90%. However, to reach this result, the magnetic fields were 1.3 T for dry separation and 0.6 T for wet separation. Therefore, the decision between dry or wet magnetic separation for the spiral concentrate should consider the magnetic separation equipment costs versus adding and removing water to the process.

All the same, dry magnetic separation showed superior performance for the shaking table concentrate than did the wet separation. At the highest tested field (1,3 T), the Sn grade increased from 39.24% to 57.21%, with Sn recovery of 87.33%. This result is similar to the Frantz separator's, indicating that dry magnetic separation was performed satisfactorily (Figure 5).

Table 4 shows the results of using a scavenger step at the magnetic product at 0.6 and 1.2 from wet magnetic separation (Figure 3B). The scavenger reduced the Sn loss as its content significantly increased from the magnetic

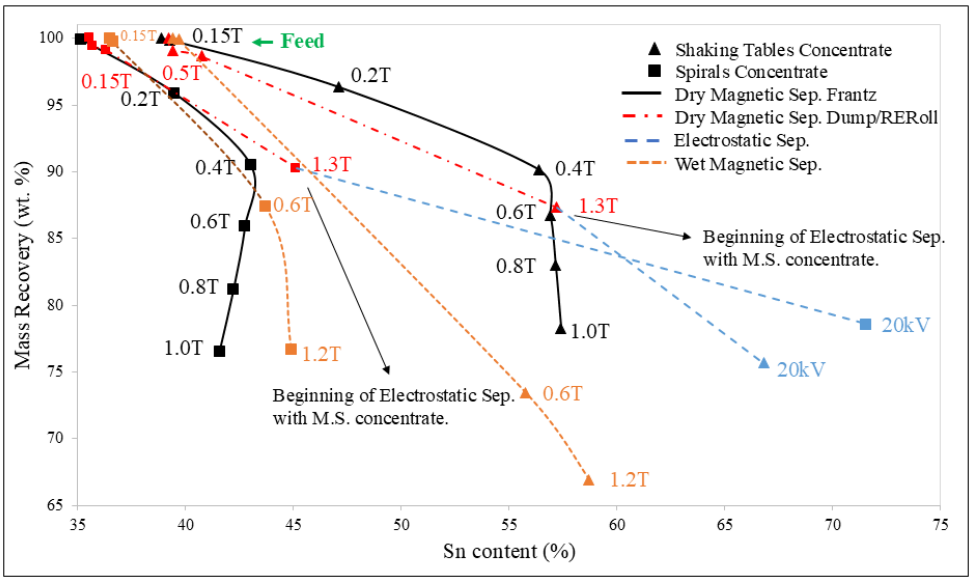

Figure 5. Performance of concentration in terms of recovery versus Sn content.

Table 4. Results of the scavenger concentration in the magnetic product of circuit B

	Shaking Tables		Spiral	
	Sn (%)	Recovery (%)	Sn (%)	Recovery (%)
Magnetic product at 0.6 T (scavenger feed)	22.07	26.48	17.06	12.35
Magnetic product of the scavenger at 0.6 T	19.81	18.77	11.00	4.55
Nonmagnetic product of the scavenger at 0.6 T	30.56	7.70	25.14	7.80
Magnetic product at 1.2 T (scavenger feed)	36.84	6.49	36.80	10.75
Magnetic product of the scavenger at 1.2 T	31.25	4.19	31.51	6.15
Nonmagnetic product of the scavenger at 1.2 T	54.60	2.30	47.44	4.61

product to the scavenger nonmagnetic product. For the shaking table concentrate, for instance, the Sn increased from 26.84 in the magnetic product at 1.2 T to 54.60% in the scavenger nonmagnetic product. The scavenger mass recoveries are low (2 to 7%), but this effect can be mitigated by recirculating products in the circuit. This result indicates that more complex circuits can improve the performance of wet magnetic separation.

The superior performance of wet magnetic separation agrees with some works in the literature. For instance, Abd El-Rahman [14] proposed wet separation to recover cassiterite from ultrafines after concentration in a Falcon centrifugal concentrator using 1.2 T. The yielded concentrate presented 68.52% of Sn with 95% recovery. Sreenivas et al. [7] combined gravity concentration with shaking tables to magnetic separation at low (0.1 T) and high (1.4 T) intensity and achieved a concentrate with 82.6% cassiterite content and 71.1% recovery

The electrostatic separation after dry magnetic separation (Figure 5) contributed to the Sn content increase from 57.21% to 66.82% for the shaking table concentrate and from 45.15% to 71.54% for the spiral concentrate, with recoveries of 75.67% and 78.60%, respectively. The optimization of concentration by adding electrostatic separation to the process agrees with Campos and Delboni [12] and Sreenivas et al. [7]. The major contribution of electrostatic separation to the spiral concentrate was its ability to reduce a large amount of Al and Si-bearing minerals, most likely quartz, zircon, and topaz.

A detailed mineralogical analysis of the concentration products must be conducted to better understand the separation of the different valuable minerals. For instance, Zhang et al. [15] reported that cassiterite presents compact embedding and fine-grained distribution in iron-bearing minerals and gangue, interfering with its processing. According to Buchmann et al. [13], this fine-disseminated feature was the main reason why cassiterite was reporting to the magnetic product and that these losses could be reduced by additional comminution.

Another analysis to be performed is the increase in temperature of the heavy mineral concentrates before the magnetic separation process. According to Banerjee [17] some cassiterites may have ferromagnetic properties due to Fe impurities in their crystal structure, which would reduce the efficiency of magnetic separation in tin concentration. In Rondônia there is evidence of the occurrence of magnetic

Table 5. Relevant oxide contents in the magnetic tailings

Final Tailings	Feed	Contents (%)				Recoveries (%)			
		TiO_2	Fe_2O_3	Nb_2O_5	Ta_2O_5	TiO_2	Fe_2O_3	Nb_2O_5	Ta_2O_5
Mag. Sep. Frantz	Tables	15.70	22.29	26.19	3.49	94.21	96.28	98.36	96.15
Mag. Sep. Drum	Tables	15.83	26.92	28.71	3.71	89.29	91.10	94.90	91.75
Mag. Sep. Frantz	Spiral	14.13	22.47	22.00	2.96	89.95	93.19	97.65	95.46
Mag. Sep. Drum	Spiral	14.58	31.01	24.74	3.35	83.91	89.33	96.02	92.92

Table 6. Relevant oxide contents in the non-conductive tailings

Final Tailings	Feed	Contents (%)			Recoveries (%)		
		Al_2O_3	SiO_2	ZrO_2	Al_2O_3	SiO_2	ZrO_2
Electro. Sep.	Tables	14.81	13.53	16.59	80.16	68.76	61.18
Electro. Sep.	Spiral	38.25	24.52	7.17	94.55	89.11	74.71

cassiterites [11]. This could be avoided by increasing the concentrate feed temperature of the concentrate, using Curie's principle (Curie's Point) to interrupt the magnetism in cassiterite [17,18].

Tables 5 and 6 show the main oxide contents in the magnetic fraction of the dry magnetic separations (drums, roll, and Frantz) and the non-conductive fraction of the electrostatic separation. In the magnetic fraction, the Ti and Nb contents ranged from 14.13% to 15.83% for the shaking table and from 22.00% to 28.71% for the spiral concentrates, indicating some level of ilmenite and columbite concentration.

Such elements have commercial value and could be treated as by-products of cassiterite processing. Then again, the non-conductive fraction showed elevated levels of Al and Si, with no concentration of elements of interest.

The Zr presents high levels in the non-conductive fraction of the shaking table concentrate (16.59%), which may have commercial value if separated from the Al and Si oxides.

4 Conclusion

The magnetic and electrostatic separations efficiently increased the Sn content in the cassiterite concentrates produced by shaking tables and spirals. Dry magnetic separation, followed by electrostatic separation, was more efficient in the Sn concentration and produced a magnetic tailing rich in Nb and Ti.

Dry magnetic separation raised the tin content from 39.24% to 57.21%, with a recovery of 87.33% in the shaking table concentrate, and from 35.57% to 45.15%, with a recovery of 90.23% in the spiral concentrate. After electrostatic separation, the Sn content rose to 66.82%, with a 75.67% recovery for the shaking table concentrate and 71.54% for the spiral concentrate, with a 78.60% recovery. In addition, electrostatic separation had a relevant contribution to removing aluminosilicates.

The magnetic tailings, resulting from the dry magnetic separation process, showed higher levels of Nb and Ti (28.71% and 15.83%, respectively). Therefore, they can be used as by-products of cassiterite mineral processing.

Acknowledgements

The authors thank the Laboratory of Mineral Processing and Laboratory of Technological Characterization of the Polytechnic School of the University of São Paulo (USP) and the Mineral Processing Research Group (GPPM) of the Federal University of Alfenas (UNIFAL-MG), where the experiments were conducted. We would also like to thank the Specialization Course in Mineral Engineering (CEEM) of UNIFAL-MG, in which this project was presented as a final research paper.

References

1 Guimarães FS, Oliveira ALR, Amorim LED, Rios FJ, Lehmann B, Hernández CR, et al. Lithium-mica composition as pathfinder and recorder of Grenvillian-age greisenization, Rondonia Tin Province, Brazil. Chemie der Erde. 2021;81(2):125737. http://doi.org/10.1016/j.chemer.2020.125737.

2 Debowski BP, Alves MI, Santos AC, Tavares AD Jr, Geraldes MC. Contribution to the understanding of the Rondonia Tin Province granites (SW Amazonian Craton) origin using U-Pb and Lu-Hf in zircon by LA-ICPMS: implications to A-type granite genesis. Journal of the Geological Survey of Brazil. 2019;3(3):151-164. http://doi.org/10.29396/jgsb.2019.v2.n3.2.

3 Lamarão CL, Marques GT, Oliveira DC, Costi HT, Borges RMK, Dallagnol R. Morphology and composition of zircons in rare metal granites from Brazilian tin provinces. Journal of South American Earth Sciences. 2018;84:1-15. http://doi.org/10.1016/j.jsames.2018.03.003.

4 Bettencourt JS, Tosdal RM, Leite WB Jr, Payolla BL. Mesoproterozoic rapakivi granites of the Rondônia Tin Province, southwestern border of the Amazonian craton, Brazil—I. Reconnaissance U–Pb geochronology and regional implications. Precambrian Research. 1999;95:41-67. http://doi.org/10.1016/S0301-9268(98)00126-0

5 Payolla BL, Bettencourt JS, Kozuch M, Leite WB Jr, Fetter AH, Van Schmus WR. Geological evolution of the basement rocks in the east-central part of the Rondônia Tin Province, SW Amazonian craton, Brazil: U–Pb and Sm-Nd isotopic constraints. Precambrian Research. 2002;119(1-4):141-169. http://doi.org/10.1016/S0301-9268(02)00121-3.

6 Bowles JFW. Cassiterite. In: Alderton D, Elias SA, editors. Encyclopedia of geology. 2nd ed. Oxford: Elsevier; 2021.

7 Sreenivas T, Srinivas K, Natarajan R, Padmanabhan NPH. Padmanabhan. Na integrated process for the recovery of tungsten and tin from a combined wolframite-scheelite-cassiterite concentrate. Mineral Processing and Extractive Metallurgy Review. 2004;25(3):193-203. http://doi.org/10.1080/08827500490441332.

8 Wills BA, Atkinson K. Some observations on the fracture and liberation of mineral assemblies. Minerals Engineering. 1999;6(7):697-706. http://doi.org/10.1016/0892-6875(93)90001-4.

9 Wright PA. Extractive metallurgy of tin. 2nd ed. New York: Elsevier Scientific Publishing Company Press; 1982.

10 Sampaio JA, Luz AB, France SCA, Gonzaga LM. Separação magnética e eletrostática. In: Centro de Tecnologia Mineral, editor. Tratamentos de minérios. 6ª ed. Rio de Janeiro: CETEM/MCTIC; 2018. p. 341-379 [cited 2023 Feb 15]. Available at: http://mineralis.cetem.gov.br/handle/cetem/2180

11 Buch T, Marbler H, Haubrich F, Trinkler M. Investigation of tin and tantalum ores from the Rondônia Tin Province, northern Brazil, to develop optimized processing technologies. Porto Velho: CPRM; 2018. Report [cited 2022 Dec 25]. Available at: https://rigeo.cprm.gov.br/handle/doc/20331

12 Campos JA, Delboni H Jr. Utilização de separadores magnéticos de alta intensidade e eletrostáticos na concentração columbita-tantalita e cassiterita. In: Proceedings of the XIX National Meeting on Ore Treatment and Extractive Metallurgy; 2002; Recife, Brazil. Rio de Janeiro: CETEM; 2002. p. 358-364.

13 Buchmann M, Schach E, Tolosana-Delgado R, Leißner T, Astoveza J, Kern M, et al. Evaluation of magnetic separation efficiency on a cassiterite-bearing skarn ore by means of integrative SEM-based image and XRF–XRD data analysis. Minerals. 2018;8(9):390. http://doi.org/10.3390/min8090390.

14 Abd El-Rahman MK, Youssef MA, Helal NH, El-Rabiei MM, Elsaidy SR. Experimental design technique on recovery of fine cassiterite from Igla placer ore of Egypt. The Journal of Ore Dressing. 2009 [cited 2023 Nov 21];11:24-32. Available at: https://www.researchgate.net/profile/El-Sayed-Hassan-2/publication/269159285

15 Zhang Y, Wang J, Cao C, Su Z, Chen Y, Lu M, et al. New understanding on the separation of tin from magnetite-type, tin-bearing tailings via mineral phase reconstruction processes. Journal of Materials Research and Technology. 2019;6(6):5790-5801. http://doi.org/10.1016/j.jmrt.2019.09.048.

16 Mattioli MV. Caracterização mineralógica do rejeito magnético (Pilha 2) da frente de lavra Gilberto Kubotani, Mina Bom Futuro, Rondônia [monografia]. Rio Claro: Universidade Estadual Paulista "Júlio de Mesquita Filho"; 2022.

17 Banerjee SK. Origin of weak ferromagnetism and remanence in natural cassiterite crystals. Journal of Geophysical Research. 1969;74(15):3789-3795. http://doi.org/10.1029/JB074i015p03789.

18 Grubb PLC, Hannaford P. Magnetism in cassiterite. Mineralium Deposita. 1969;1(2):148-171. http://doi.org/10.1007/BF00206184.

Received: 31 Jul. 2024
Accepted: 12 Nov. 2024

Editor-in-charge: André Carlos Silva